

SEMI-EMPIRICAL HAMILTONIAN MODEL FOR ELLIPTICAL CAVITIES

E. Laface*, J. F. Esteban Müller, European Spallation Source ERIC, Lund, Sweden

Abstract

We propose to use the sum of TM_{0m0} modes to treat a radio-frequency superconducting elliptical cavity as a pill-box cavity with variable radius. The amplitudes of the different modes are obtained interpolating the field-map of the cavity with the model. Once the field is calculated, the Hamiltonian of the cavity is constructed and used to evaluate the transfer matrices associated to each step of the field-map. The multi-particle non-linear dynamics can also be evaluated using the Lie Transform of the Hamiltonian. The results are benchmarked against the ESS Linac Simulator contained in the OpenXAL suite.

INTRODUCTION

The beam dynamics models used to track charged particles in radio-frequency (RF) cavities can be summarized in two families: the analytical model based on the so-called pill-box solution [1] and the field-map models based on the numerical solution of the Poisson equation within the RF cavity [2].

The pill-box model is useful to have an overview of the behaviour of the cavity but it is developed considering that the cavity is a cylinder with a constant aperture. Many RF cavity designs, like for example the elliptical cavity, have a complicate shape with variable radius. This implies that the pill-box model will not be very accurate in representing such cavities. On the other hand, the field-map model reproduces correctly the field into the cavity but it lost the possibility to do some analytic consideration about the nature of the solution because the result is purely numeric.

In this paper we extend the pill-box cavity model considering additional TM modes. This new model is more accurate in reproducing the field-map, while still analytic. The Hamiltonian of the system can be calculated and solved with linear (paraxial approximation) and non-linear (Lie methods [3]) techniques.

For the purpose of this paper, we considered the Medium- β superconducting RF cavity designed for the European Spallation Source proton Linac. This is a cavity operating at the frequency of 704.42 MHz and it is 1.5 m long [4].

THE FIELD MODEL

Radial Dependency of E_z

The idea of this model starts from the observation that the electric field in the elliptical cavity is very close to the one of pill-box at the entrance of the cavity but it diverges from it when observed in the middle of the gaps. The latter shape seems generated by additional TM_{0m0} electromagnetic

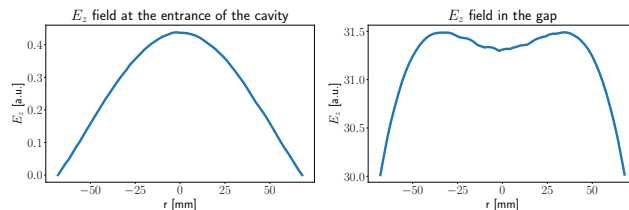


Figure 1: Left: the electric field at the entrance of the cavity is reproducible with a simple $J_0(kr)$ Bessel function. Right: in the elliptical gap the field shows additional modes.

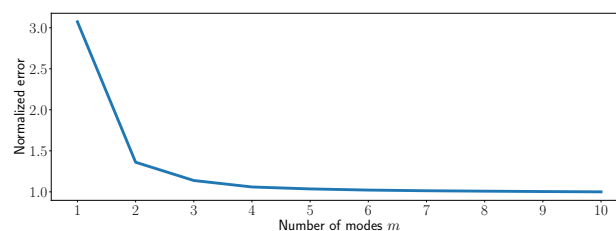


Figure 2: Normalized distance between the model and the field-map vs. the number of modes m .

modes that emerge because of the change in the aperture of the cavity (Fig. 1).

The first step is then to fit the radial component of the longitudinal electric field E_z with the function,

$$E_z = \sum_{i=1}^m E_{i,s} J_0 \left(p_{0i} \frac{r}{a_s} \right), \quad (1)$$

where the index i runs on the modes considered; $E_{i,s}$ is the amplitude of each mode in the position s , p_{0i} is the zero of the i -th mode of the Bessel function J_0 ; r is the distance from the center of the cavity and a_s is the aperture at the s position. To split the cavity we use the steps of the field-map mesh that are 375, so one slice every 4 mm. It is useful here to recall that the variable z is used as the distance of a particle from the reference particle, while the coordinate s is the distance from the entrance of the cavity.

To establish how many modes we need to include in order to fit the cavity we tried values of m from 1 to 10 and we evaluated the square root of the difference between the field-map and the fit model. The result is normalized at the value obtained for the order $m = 10$.

The dependence of the error from the number of modes is in Fig. 2. Here it is possible to see that the distance of the model from the field-map converges quickly and we decided, for the rest of this study, to consider the modes up to $m = 5$ because the reduction in the error due to higher order modes does not justify the additional computational time.

* Emanuele.Laface@ess.se

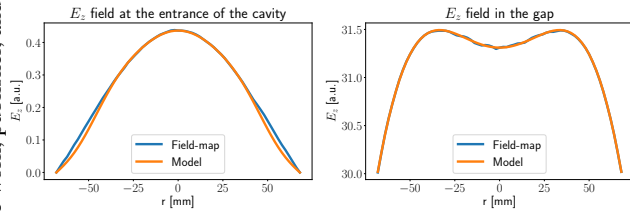


Figure 3: Electric field at the entrance of the cavity (left) and in the elliptical gap (right). Field-map vs. model.

Time Dependence of E_z

The field in Eq. (1) takes into account only the radial dependence of E_z but the field oscillates also in time. If the amplitude coefficients $E_{i,s}$ were constant, we should consider five time frequencies, one for each TM mode, in order to find a proper solution of the Maxwell equations. However, in our case, the coefficients change for each step were considered in a way that is obtained empirically matching the model with the field-map.

Therefore, we do not have a closed solution, but we can exploit the fact that our model is reproducing the field-map, and we know that the field-map is designed to have only one time frequency. Then we can assume that our field will be:

$$E_z = \left[\sum_{i=1}^m E_{i,s} J_0 \left(p_{0i} \frac{r}{a_s} \right) \right] \sin(\omega t + \phi_0), \quad (2)$$

where ω is the frequency of the cavity and ϕ_0 is the working phase chosen for the reference particle. A technique used to treat the time dependence of the field, the so-called transit-time factor (TTF), is to integrate the field over the time for each gap of the cavity. In our model we have the cavity split in 4-mm slices, so we can calculate the time variation of the field for each slice instead of using the TTF. To do so it is convenient to apply a coordinate transformation from t to s using the velocity of the reference particle β_0 as

$$\omega t = \frac{\omega}{c} \left(\frac{s}{\beta_0} - z \right). \quad (3)$$

The final model for E_z that we will use is

$$E_z = \left[\sum_{i=1}^m E_{i,s} J_0 \left(p_{0i} \frac{r}{a_s} \right) \right] \sin \left[\phi_0 + \frac{\omega}{c} \left(\frac{s}{\beta_0} - z \right) \right], \quad (4)$$

remembering that the reference velocity and phase β_0 and the ϕ_0 changes for each slice because the particle accelerates so we have to adjust the velocity according to the increase of energy.

The comparison of the field-map with the model calculated with the Eq. (4) at the entrance and in one gap of the cavity can be seen in Fig. 3, while in Fig. 4 it is possible to see the full electric field in the cavity for the field-map and for the model.

THE HAMILTONIAN

Once we have an analytic model for the electric field (Eq. 4) we have the possibility to write a Hamiltonian and

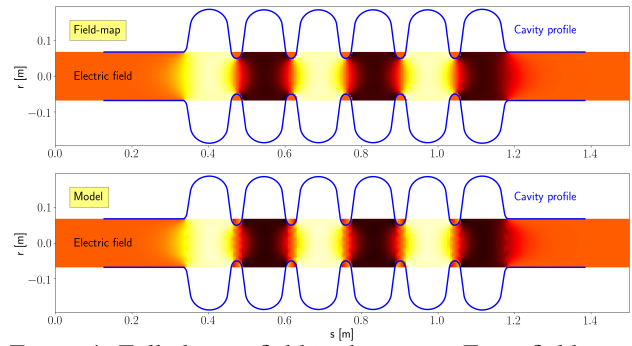


Figure 4: Full electric field in the cavity. From field-map (top) and calculated with the model (bottom).

solve it in order to calculate the dynamics of the particles. The first step is to identify a potential that can generate the electric and magnetic fields. We will use the treatment described in Chapter 3.6 of [5]. The potential vector is given by:

$$A = \left(0, 0, \frac{c}{\omega} \left[\sum_{i=1}^m E_{i,s} J_0 \left(p_{0i} \frac{r}{a_s} \right) \right] \cos \left[\phi_0 + \frac{\omega}{c} \left(\frac{s}{\beta_0} - z \right) \right] \right) \quad (5)$$

and the Hamiltonian, again from Ref. [5], is

$$H = \frac{\delta}{\beta_0} - \sqrt{\left(\delta + \frac{1}{\beta_0} \right)^2 - p_x^2 - p_y^2 - \frac{1}{\beta_0^2 \gamma_0^2}} - \frac{qc}{P_0 \omega} \left[\sum_{i=1}^m E_{i,s} J_0 \left(p_{0i} \frac{r}{a_s} \right) \right] \cos \left[\phi_0 + \frac{\omega}{c} \left(\frac{s}{\beta_0} - z \right) \right] \quad (6)$$

where δ , p_x and p_y are the longitudinal, horizontal and vertical momenta with respect to the reference particle; q is the charge and P_0 is the momentum of the reference particle.

The Linear Solution

Given the Hamiltonian 6 we can apply the paraxial approximation expanding the Hamiltonian at the second order around the reference particle. For each slice s we have

$$H = \frac{\delta^2}{2\beta_0^2 \gamma_0^2} + \frac{p_x^2}{2} + \frac{p_y^2}{2} + \sum_{i=1}^m \left[E_{i,s} \left(\frac{p_{0i}}{a_s} \right)^2 \right] \frac{qc}{4P_0 \omega} \cos \left(\phi_0 + \frac{\omega s}{\beta_0 c} \right) (x^2 + y^2) + \sum_{i=1}^m (E_{i,s}) \frac{\omega q}{2P_0 c} \cos \left(\phi_0 + \frac{\omega s}{\beta_0 c} \right) z^2 - \sum_{i=1}^m (E_{i,s}) \frac{q}{P_0} \sin \left(\phi_0 + \frac{\omega s}{\beta_0 c} \right) z. \quad (7)$$

The solution of this Hamiltonian is a transfer matrix M for the quadratic component, plus a vector that shift the longitudinal momentum and energy of the reference particle

due to the acceleration. Substituting

$$\xi = \sqrt{\sum_{i=1}^m \left[E_{i,s} \left(\frac{p_{0i}}{a_s} \right)^2 \right] \frac{qc}{2P_0\omega} \cos \left(\phi_0 + \frac{\omega s}{\beta_0 c} \right)} \quad (8)$$

$$\zeta = \sqrt{\sum_{i=1}^m (E_{i,s}) \frac{q\omega}{P_0 c} \cos \left(\phi_0 + \frac{\omega s}{\beta_0 c} \right)}, \quad (9)$$

the transfer matrices separated by coordinates are

$$M_{x,y} = \begin{bmatrix} \cos(L\xi) & \frac{\sin(L\xi)}{\xi} \\ -\xi \sin(L\xi) & \cos(L\xi) \end{bmatrix} \quad (10)$$

$$M_z = \begin{bmatrix} \cos\left(\frac{L}{\beta_0\gamma_0}\zeta\right) & \frac{\sin\left(\frac{L}{\beta_0\gamma_0}\zeta\right)}{\beta_0\gamma_0\zeta} \\ -\beta_0\gamma_0\zeta \sin\left(\frac{L}{\beta_0\gamma_0}\zeta\right) & \cos\left(\frac{L}{\beta_0\gamma_0}\zeta\right) \end{bmatrix}. \quad (11)$$

The matrices (10) and (11) are not sufficient to describe the dynamics of the Hamiltonian (7) because it is missing the first order term in z that is given by

$$V_{x,y} = \begin{bmatrix} 0 \\ 0 \end{bmatrix} \quad (12)$$

$$V_z = \begin{bmatrix} \left(\frac{c}{\omega} - \cos\left(\frac{L}{\beta_0\gamma_0}\zeta\right) \right) \tan\left(\phi_0 + \frac{\omega s}{\beta_0 c}\right) \\ \beta_0\gamma_0\zeta \sin\left(\frac{L}{\beta_0\gamma_0}\zeta\right) \tan\left(\phi_0 + \frac{\omega s}{\beta_0 c}\right) \end{bmatrix}, \quad (13)$$

and the dynamics after each slice of length L is given by

$$\vec{x}_L = M_x \vec{x}_0 + V_x \quad (14)$$

$$\vec{y}_L = M_y \vec{y}_0 + V_y \quad (15)$$

$$\vec{z}_L = M_z \vec{z}_0 + V_z \quad (16)$$

where the arrow means that we are taking the array with coordinate and momentum. It is important to notice here that a reference particle with $z = 0$ and $\delta = 0$ will no longer be the reference after the transport along the slice, because V_z changes both. This is correct because the formalism is expressed in the frame of a particle that doesn't change energy, while a reference particle is accelerating. This means that after each step we need to reset the reference particle to zero adjusting the value of β_0 , γ_0 and P_0 to the new energy value.

The adjustment of the momentum has also an effect on the transverse plane and it will shrink the phase space. This means that, to restore the reference particle, we have to operate as

$$\vec{x}_{P_1} = R_P \vec{x}_{P_0} \quad (17)$$

$$\vec{y}_{P_1} = R_P \vec{y}_{P_0} \quad (18)$$

$$\vec{z}_{P_1} = R_P \vec{z}_{P_0} + R_z, \quad (19)$$

where

$$R_P = \begin{bmatrix} 1 & 0 \\ 0 & \frac{P_0}{P_1} \end{bmatrix}; \quad R_z = \begin{bmatrix} 0 \\ \frac{1}{\beta_1} \left(\frac{\gamma_0}{\gamma_1} - 1 \right) \end{bmatrix}. \quad (20)$$

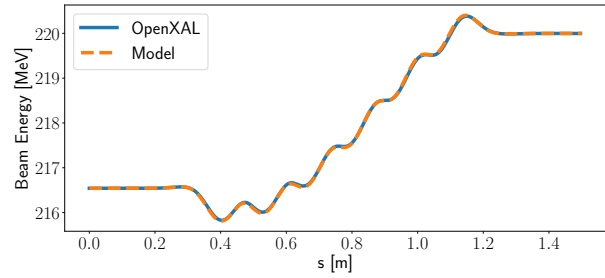


Figure 5: Energy increase in the first medium- β cavity calculated with the ESS Linac Simulator and with the model of this paper.

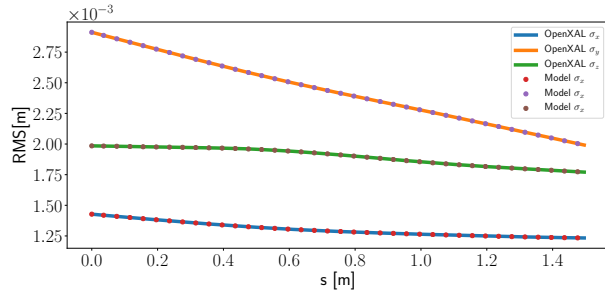


Figure 6: σ_x , σ_y , σ_z of the beam along the RF Cavity calculated with the ESS Linac Simulator and with the model of this paper.

RESULTS

In order to evaluate if this model reproduces correctly the linear dynamics we compared it with a simulation performed with the well-established code ESS Linac Simulator contained in the OpenXAL suite [6, 7]. The element of accelerator that was considered in the simulations was the first medium- β cavity of the ESS Proton Linac. The first quantity analyzed for the comparison is the beam energy. The first medium- β cavity accelerates the beam from 216.54 MeV to 219.99 MeV. The comparison between the field-map model in the ESS Linac Simulator and the model described in this paper is in Fig. 5 where it is possible to see that the two simulations are in very good agreement.

After the energy, we compared the transverse and longitudinal RMS evolution of the beam along the cavity and we plotted the results in Fig. 6. The initial conditions of the beam used for the simulations are summarized in Table 1.

Table 1: Beam Parameters at the Entrance of the Cavity

Beam current	0 mA		
Kinetic Energy	216.54 MeV		
	α	β	ϵ
x	0.715	4.245 m	0.4801e-6 m rad
y	4.350	18.103 m	0.468e-6 m rad
z	0.232	9.666 m	0.407e-6 m rad

CONCLUSIONS

We discussed a new method to represent the field-map using a Hamiltonian where the coefficients are obtained by a semi-empirical matching of the parameters with the field-map. The linearized results were successfully compared with a well established simulator proving that the method reproduces a correct beam dynamics. This technique opens the possibility to study, in the future, the non-linear beam dynamics of the RF cavity applying the Lie methods as described in [8].

REFERENCES

- [1] T. P. Wangler, *RF Linear Accelerators, 2nd, Completely Revised and Enlarged Edition*, ser. Physics textbook. Weinheim: Wiley-VCH, Jan 2008.
- [2] J. Qiang *et al.*, “An object-oriented parallel particle-in-cell code for beam dynamics simulation in linear accelerators,” *Journal of Computational Physics*, vol. 163, no. 2, pp. 434–451, 2000.

- [3] A. J. Dragt, *Lie methods for nonlinear dynamics with applications to accelerator physics*. University of Maryland, Center for Theoretical Physics, Department of Physics, 2017.
- [4] P. Michelato *et al.*, “ESS medium and high beta cavity prototypes,” in *Proceedings, 7th International Particle Accelerator Conference*, no. WEPMB011, Busan, South Korea, May 2016.
- [5] A. Wolski, *Beam dynamics in high energy particle accelerators*. London: Imperial College Press, 2014.
- [6] E. Laface *et al.*, “The ESS Linac Simulator: a first benchmark with TraceWin,” in *Proceedings, 4th International Particle Accelerator Conference*, no. TUPWO046, Shanghai, China, May 2013.
- [7] J. Esteban Müller and E. Laface, “Latest developments and updates of the ESS Linac Simulator,” in *Proceedings, 9th International Particle Accelerator Conference*, no. WEPAF086, Vancouver, Canada, May 2018.
- [8] E. Laface and J. Esteban Müller, “Self-consistent Space Charge Tracking Method based on Lie Transform,” in *Proceedings, 8th International Particle Accelerator Conference*, no. THPVA019, Copenhagen, Denmark, May 2017.